An innovative seeding technique for photon conversion reconstruction at CMS

[1]D Giordano and [2]G Sguazzoni

[1]CERN, Information Technology Department, Experiment Support Group, Geneva, Switzerland
[2]INFN, Firenze, Italy

E-mail: domenico.giordano@cern.ch, giacomo.sguazzoni@cern.ch

Abstract. The conversion of photons into electron-positron pairs in the detector material is a nuisance in the event reconstruction of high energy physics experiments, since the measurement of the electromagnetic component of interaction products results degraded. Nonetheless this unavoidable detector effect can also be extremely useful. The reconstruction of photon conversions can be used to probe the detector material and to accurately measure soft photons that come from radiative decays in heavy flavor physics. In fact a converted photon can be measured with very high momentum resolution by exploiting the excellent reconstruction of charged tracks of a tracking detector as the one of CMS at LHC. The main issue is that photon conversion tracks are difficult to reconstruct for standard reconstruction algorithms. They are typically soft and very displaced from the primary interaction vertex. An innovative seeding technique that exploits the peculiar photon conversion topology, successfully applied in the CMS track reconstruction sequence, is presented. The performances of this technique and the substantial enhancement of photon conversion reconstruction efficiency are discussed. Application examples are given.

1. Introduction

The precise and efficient determination of charged-particle momenta is a critical component of the physics program of the LHC experiments, as it impacts the ability to reconstruct leptons, charged hadrons and jets, which are the basic physics objects needed to study *pp* collisions. Achieving the necessary momentum resolution requires precise tracking in a high magnetic field. This has been obtained by the two LHC general purpose experiments adopting a design with the inner tracking systems in a solenoidal magnetic field.

What makes track reconstruction difficult is the large number of hits in the tracking detectors produced by the many tracks resulting from several *pp* interactions in the same bunch crossing. In order to mitigate this issue the hit occupancy is kept low using highly granular sensors and, consequently, a high number of electronic channels (several millions) for their front-end readout at the cost of an increase of material in the tracking volume. These channels need to be powered, controlled, and read-out through complex systems of cables and optical fibers. Moreover they have to dissipate a considerable amount of heat, hence a capillary cooling system is also required. The consequent amount of material contained in the detectors and support structures is not negligible and has an effect on the tracking performance because of multiple scattering, energy loss and electron bremsstrahlung. For this reason the track reconstruction

has to properly take into account the amount of material in the tracking volume, which has to be known with extreme accuracy. This material affects also the overall event topology and its reconstruction because of photon conversions and nuclear interactions that modify the energy flow through the inner detector.

This unavoidable detector effect can also be turned into an extremely useful tool. For instance the reconstruction of photon conversions can be used to probe the detector material and to accurately measure soft photons produced in radiative decays of heavy flavor particles.

In this paper we will discuss the impact of photon conversions in the event reconstruction at LHC. We will refer to the CMS detector [1], even if most of the concepts discussed can be applied also to other detectors. In the following sections a description of the CMS detector will be provided as well as some examples of the problems and the advantages due to the photon conversions inside the tracking volume. We will summarize the current methods for the reconstruction of photon conversions and describe an innovative additional technique that allows to increase their reconstruction efficiency.

2. The CMS detector

The Compact Muon Solenoid (CMS) detector features an all-silicon tracker, a lead tungstate crystal electromagnetic calorimeter (ECAL), and a brass-scintillator hadronic calorimeter, all contained inside a 3.8 T superconducting solenoid. The strong magnetic field enables the measurement of charged particle momenta over more than four orders of magnitude, from less than 100 MeV/c to more than 1 TeV/c, by reconstructing their trajectories as they traverse the CMS inner tracking system. The iron return yoke of the solenoid is interspersed with gas detectors that are used to identify muons.

The CMS Tracker, shown in Fig. 1, consists of 1 440 silicon pixel and 15 148 silicon strip detector modules, covering the region from 4 cm to 110 cm in radius, and within 280 cm on either side of the collision point along the LHC beam axis. The tracker acceptance extends up to a pseudo-rapidity of $|\eta| < 2.5$. The pseudo-rapidity η is defined as $-\log[\tan(\theta/2)]$, where θ is the polar angle with respect to the direction of the LHC counter-clockwise beam, and ϕ is the azimuthal angle in the plane orthogonal to the beams. The tracker detector provides an impact parameter resolution of $\sim 15\mu$m and a transverse momentum (p_T) resolution of about 1.5 % for 100 GeV/c particles. The ECAL towers are projective and finely segmented, with $\Delta\phi \sim \Delta\eta \sim 0.087$ in the central region, allowing precise reconstruction of the e/γ position and energy.

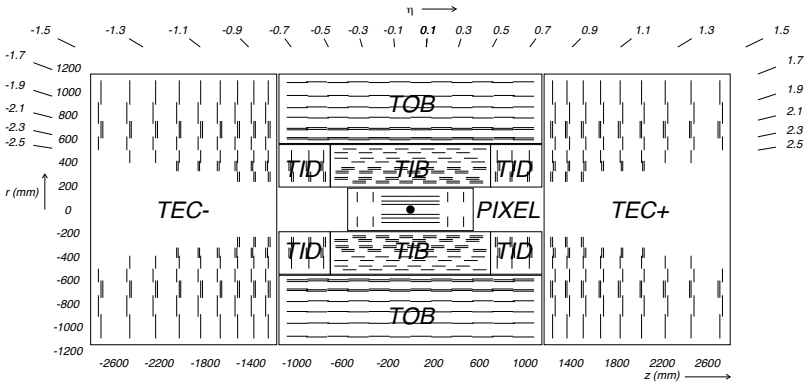

Figure 1. Schematic cross section through the CMS Tracker. Each line represents a detector module. Double lines indicate back-to-back modules which deliver stereo hits.

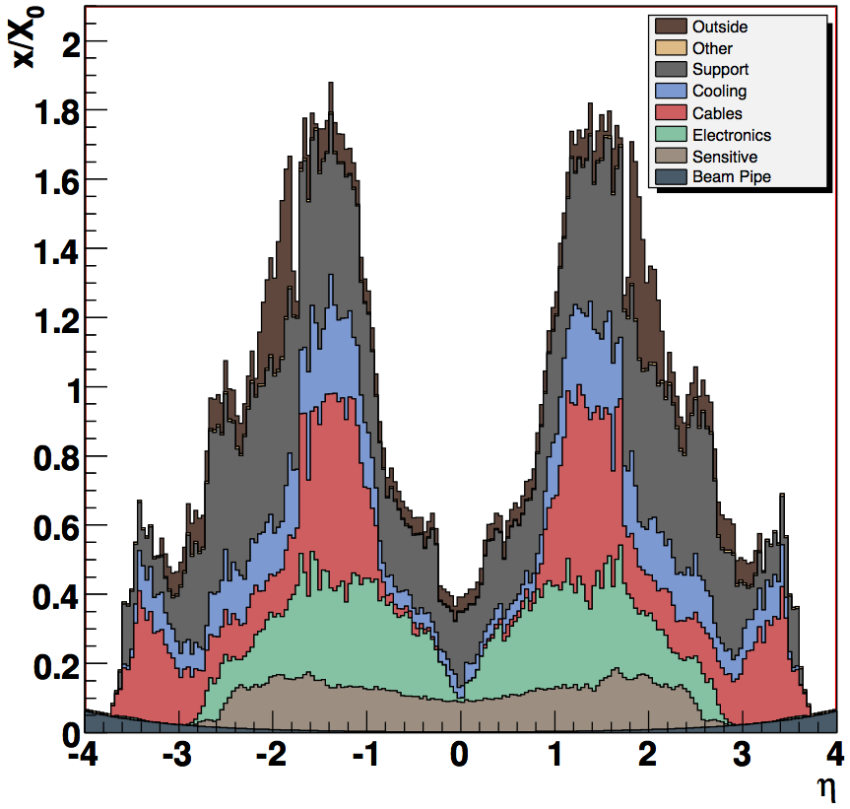

Figure 2. Material budget inside the CMS Tracker volume in units of radiation length as a function of pseudorapidity η broken down into the functional contributions.

Figure 2 shows the material budget of the CMS tracker in units of radiation length (X_0). The overall material crossed by a particle traversing the Tracker volume can exceed 1 X_0. It increases from 0.4 X_0 at $\eta \sim 0$ to about 1.8 X_0 at $|\eta| \sim 1.4$, beyond which it falls to about 1 X_0 at $|\eta| \sim 2.5$. The largest contribution to the Tracker mass is by far represented by the passive structures having the largest uncertainty on their overall amount. This uncertainty can have a sensible impact on the expected physics performance.

3. Effects of photon conversions

As a consequence of the amount of material shown in Fig. 2, up to 70% of photons traversing the CMS Tracker material convert into e^+e^- pairs, resulting in a large fraction of secondary electrons. Most of these photons are from $\pi^0 \to \gamma\gamma$ decays. Other sources are prompt photons and the photons emitted by bremsstrahlung before an electron reaches the electromagnetic calorimeter. These electron pairs are a non-negligible background to prompt electrons from *pp* collisions and must be rejected efficiently in many physics analyses whose signatures contain prompt electrons.

For this purpose CMS has developed several methods to reduce the electron fake rate by vetoing electron candidates that match one of the two tracks of a photon conversion. Some methods explicitly identify photon conversions, others use information contained in the electron candidate, such as the hit-pattern to infer if the track is prompt or not from the number of inner missing hits.

Converted photons inside jets can affect the jet energy measurement or lead to jet mis-identification, if not properly reconstructed. For instance, a leading π^0 carrying most of the

momentum of the jet can decay in two photons such that one photon exhibits the majority of the π^0 energy. If that photon then converts in the tracker material in an asymmetric fashion, such that an electron carrying most of the photon energy is produced, the electron track will match to the rest of the jet electromagnetic energy deposition, resulting in a misidentification of the genuine jet as an electron. Given the asymmetrical distribution of the energy among the two particles in the e^+e^- pair, the not-leading track can have a very low p_T and/or a very displaced vertex making its reconstruction inefficient. The same challenge subsists for the reconstruction of soft-p_T photon conversions ($\lesssim$ 3 GeV/c) some of which do not even reach the electromagnetic calorimeter.

Another field of interest is the reconstruction of prompt photons as a signature of physic in studies like $H \to \gamma\gamma$. These photons have in general high-p_T (above 10 GeV/c) and even if they undergo conversion they can be reconstructed by the electromagnetic calorimeter, as far as both tracks deposit their energy inside the calorimeter. However for many analyses it is essential to be able to reconstruct converted photons through the two produced tracks, to profit from the higher angular resolution of these tracks, in order to better associate the primary vertex from which the original photon belongs.

Other than the drawbacks of photon conversions described above, this phenomenon can be reverted in favor of specific and cutting-edge applications, such as the accurate measurement of the material inside the tracker volume, an aspect that is crucial to have a realistic material description in the track reconstruction, or the spectroscopy of excited states of heavy flavor particles decaying radiatively.

A robust method for the material budget estimation, exploited also by many past experiments [2], is based on photon conversions [3]. Conversion vertices are reconstructed with a typical radial resolution of $\sigma_r = 0.2$ to 0.5 cm and angular resolution of 1 mrad, primarily as a function of pseudo-rapidity. The idea is that the material radiography, provided by the position of reconstructed photon conversion vertices, allows for the visualisation of detector layers and service structures and that the conversion rate provides an estimate of the amount of material in the detector volume in terms of radiation lengths. In Fig. 3 the position of conversion vertices reconstructed in CMS data is shown in the (x, y) plane: in Fig. 3(a) the structure at the very centre is the Pixel detector, surrounded by the shell and rails supporting the Pixel detector, four layers of the Inner Tracker and the first layer of the Outer Tracker. When restricting the (x, y) view to $\pm$12 cm, Fig. 3(b), the beam pipe is clearly visible, off-centered with respect to the Pixel detector. The (z, r) view of conversion vertices reconstructed in data is shown in Fig. 4; the less populated areas around $|\eta| \sim 1.2$ corresponds to transition regions between the Tracker barrel and endcap sub-components where the larger amount of passive material and the change in the active material topology makes more difficult the reconstruction of displaced vertexes. The dedicated seeding described in Sec. 5 provides a reasonable increase of efficiency, as it will be shown later.

Another field that takes advantage of the photon conversion reconstruction is the study of heavy quarkonia states. These bound states of charm and bottom quark-antiquark pairs play an important role in the detailed understanding of quantum-chromodynamics (QCD), the theory describing the strong interactions among elementary particles. A quantitative understanding of the mechanisms of quarkonium production can be provided by measurements of the production cross sections and polarizations of P-wave quarkonia, such as the χ_{cJ} and the χ_{bJ} states, especially at the high transverse momentum ranges reachable in high-energy proton colliders. The CMS experiment is well capable of detecting and accurately reconstructing the χ_c and χ_b states, through their radiative decays to the J/ψ and Υ state respectively, with the low-energy photons being detected through their conversion in electron-positron pairs [4].

At low energies the calorimetric measurements do not have precisions comparable to those obtainable when the photon energy is measured through the tracking of the electron-positron

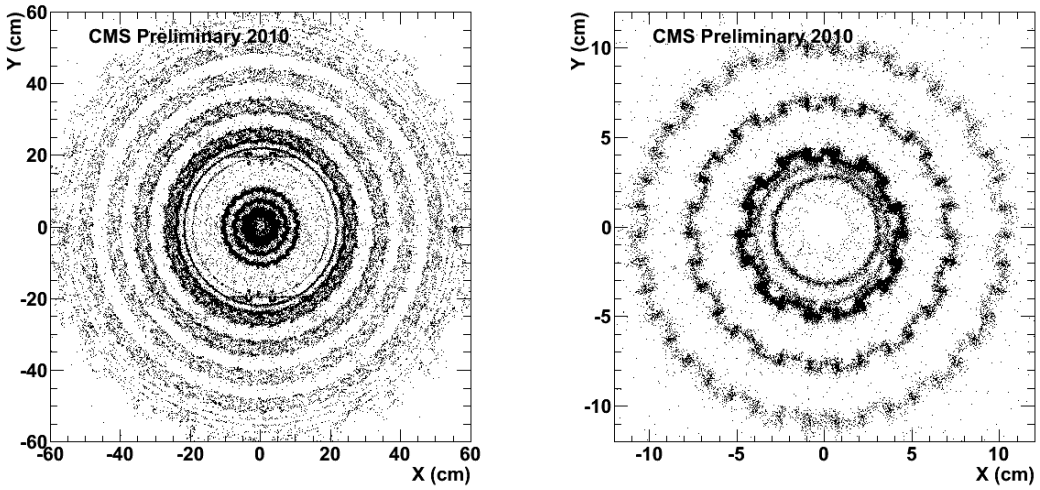

(a) (b)

Figure 3. Conversion vertices reconstructed in CMS data in the (x, y) plane for $|z| < 26\,\text{cm}$; zoom increases from (a) to (b). Results were obtained on a sample corresponding to 1/nb of integrated luminosity where about 260 000 photon conversions were reconstructed.

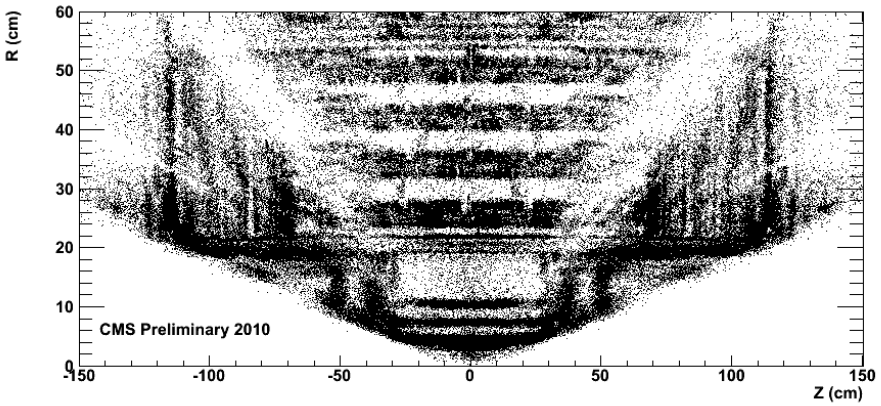

Figure 4. Conversion vertices reconstructed in CMS data in the (z, r) plane.

pair originating from a conversion of the photon. Figure 5 shows the invariant mass distribution for χ_c candidates observed through their radiative decay in $\mathrm{J}/\psi + \gamma$. The excellent momentum resolution of the reconstructed photon conversions translates in a mass resolution of less then 10 MeV/c^2, what is enough to disentangle the states χ_{c1} and χ_{c2}, whose masses differ by only $45\,\text{MeV}/c^2$. Furthermore, the converted photons have an accurate assignment of the interaction vertex where they come from, allowing to limit the combinatorial background in the invariant mass spectrum of Fig. 5 rejecting wrong combinations of dimuons plus photons produced in different *pp* collisions at the same bunch crossing (something especially important in the presence of a large number of pileup collisions).

The drawback of the usage of photon conversions for a physics measurement is the reduced yield caused by the low efficiency of their reconstruction as pairs of low momentum tracks

displaced with respect to the beam axis. Typical efficiency is of the order of 0.1 to 5% for photon $p_T < 5\,GeV/c$. It is then evident that any new algorithm contributing to increase this efficiency has a direct impact in the physics analyses.

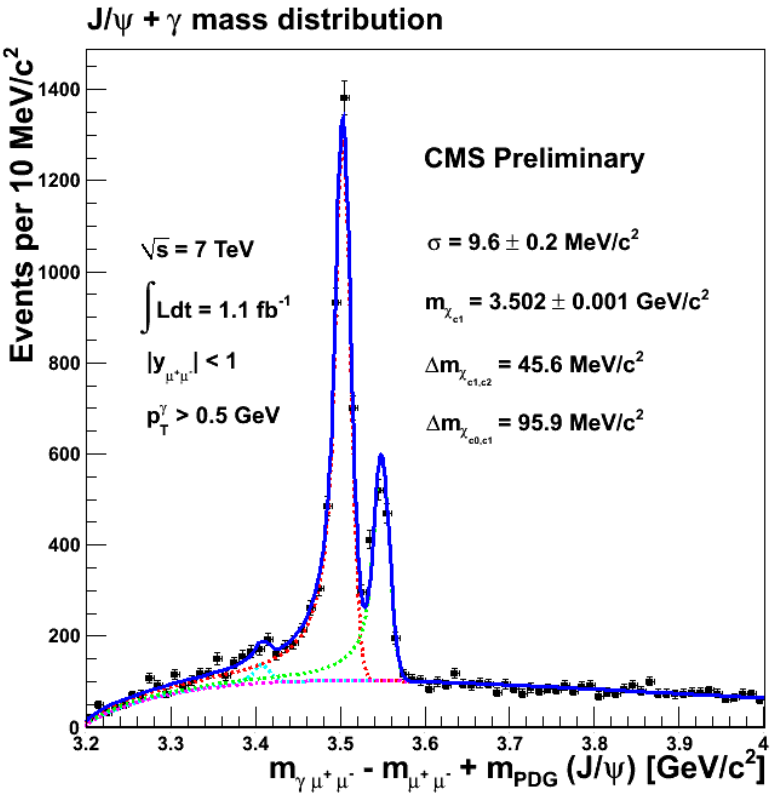

Figure 5. Invariant mass spectrum for χ_{c1} ($m_{PDG} = 3.510\,GeV/c^2$) and χ_{c2} ($m_{PDG} = 3.556\,GeV/c^2$) candidates reconstructed through their radiative decay to $J/\psi + \gamma$.

4. Photon conversion reconstruction

Reconstruction of converted photons is therefore a crucial step in the physics program of CMS, and algorithms have been developed, which exploit the conversion pair signature to distinguish genuine pairs from fake pairs. The general reconstruction approach is to preselect pairs of oppositely charged tracks satisfying the quality and topological criteria of photon conversions and to fit each of these pairs by a 3D-constrained kinematic vertex fitter that imposes the two tracks to be parallel at the vertex.

Two methods are used in CMS to generate the collection of potential conversion tracks: the ECAL-seeded conversion method [5] and the combined conversion method. The former starts from calorimetric clusters and is optimized for very displaced conversion vertexes as well as high-p_T photons ($p_T > 10\,GeV/c$). To reconstruct photon conversions within a soft-p_T spectrum (such as the majority of the photons from π^0 decays in minimum bias events or from quarkonia excited states) the ECAL cluster-driven track cannot be used, because the electron pairs from conversions are very unlikely to reach the electromagnetic calorimeter. Therefore conversions need to be reconstructed pairing tracks from the CMS general track and electron track collections. The general track collection is an inclusive collection of tracks resulting from an

iterative procedure [6] to incorporate increasingly displaced and/or low-p_T tracks. The collection of tracks in the combined conversion method is obtained from a combination of general tracks, conversion ECAL-seeded tracks and electron tracks.

5. Tracking algorithm for photon conversions

The standard CMS tracking is made of consecutive iterative steps designed to obtain high efficiency and low fake rate for tracks coming either from the primary vertex or from displaced decay vertices while maintaining the overall computing time within the requirements of the CMS offline reconstruction. Because of this constraint, the standard implementation is not optimal to reconstruct with high efficiency tracks from photon conversions since the cuts applied in the standard reconstruction are too tight for these processes. Those tracks have usually very low momentum and, especially for displaced vertices at large radii, they have a large transverse impact parameter.

Beside the soft-p_T spectrum of the majority of the photons produced at LHC, another reason why the conversion tracks have low momentum is the asymmetric distribution of the energy among the e^+e^- pairs [7], implying that one lepton carries most of the photon energy, leaving the second lepton with a too low momentum to be reconstructed. As a result these photons are not found by the conversion finding algorithms because one of the two tracks is missing, whereas the leading track has been reconstructed.

Exploiting this feature, we have developed a dedicated track reconstruction that recovers those photon conversions for which the leading track has been already reconstructed. The leading track is used to drive the reconstruction of the second track, for this reason we refer to the algorithm as track-driven and to the leading track as the seeding track.

Our tracking algorithm is configured as an additional step of the CMS iterative tracking. Having to use all the available reconstructed tracks, it is the last to run after all the other standard iterative tracking steps. Similarly to the other steps, the track-driven algorithm starts from identifying trajectory seeds from which to build the full trajectories using the standard CMS tracking sequence, based on the Kalman filter method in the pattern recognition and track refitting. Trajectory seeds are built from pairs of hits in the Pixel and/or in the Strip Tracker detectors. In order to reduce the number of hits to combine as well as to avoid to reconstruct already built tracks, only hits not associated to other tracks are used in the seeding search.

Due to the massless photon, the tracks of the resulting electrons from a photon conversion are parallel to each other at the conversion vertex, and open in two opposite arcs of circumference in the plane transverse to the CMS magnetic field ((x, y) plane in Fig. 6 (a)), whereas they remain parallel in the longitudinal plane ((z, r) plane in Fig. 6 (b)). This is a unique feature that is the basis of the algorithm we developed.

Not all the tracks from the standard collection are used to drive our seeding. The seeding tracks are selected applying the geometrical conditions imposed by the hypothesis of belonging to a prompt-photon conversion. As described in Fig. 6 (a), in the transverse plane the photon direction (VC) is tangent to both tracks in the conversion point C. Starting from a track and its associated primary vertex (V), with pure geometrical considerations the estimated position of the conversion vertex (C) is obtained. Given that a photon conversion happens in the material inside the tracker volume, from the beampipe onwards, tracks compatible with the conversion hypothesis cannot have the estimated vertex position (C) at a radial distance from the beamline (r_C) inferior to the radius of the beampipe ($r = 3$ cm). Applying this condition, with a tollerance of 0.5 cm to take into account the resolution of our geometrical estimation, prompt tracks from primary vertices are rejected, and only potential candidates from conversions are kept.

With the same approach, for a given seeding track having the estimated position of the conversion vertex at r_C only the pairs of consecutive layers located at a radial distance from the beamline above r_C are used to build the hit pair seeds. Having to reconstruct a track of

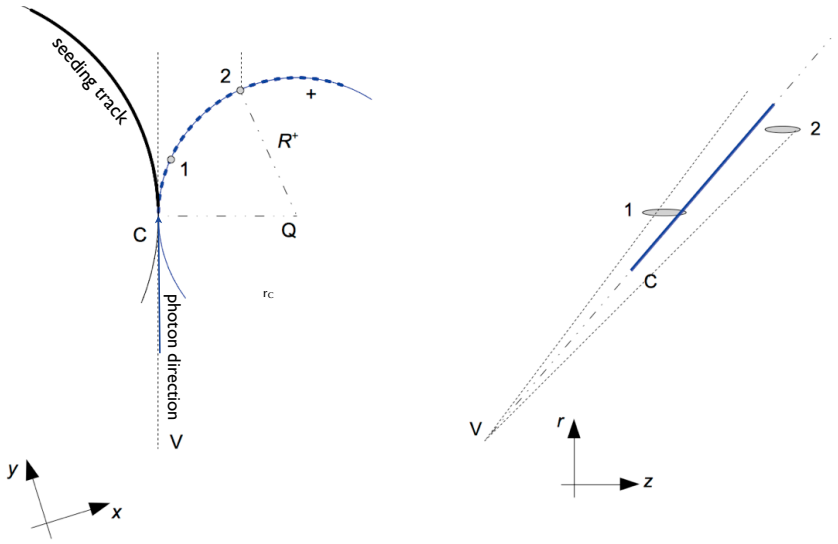

(a) (b)

Figure 6. Cartoon showing the photon conversion topology in a solenoidal magnetic field in the plane transverse to the CMS magnetic field (a), as well as in the longitudinal plane (b).

opposite charge with respect to the seeding track, only hit pairs in the semi-plane defined by the VC direction and opposite to the seeding track are considered. The search is limited to an maximum opening angle – with respect to the direction VC – correlated to the minimum p_T to be reconstructed, that in our case is 100 MeV/c.

The requirement that the two conversion tracks are parallel to the photon direction in the (z, r) plane (Fig. 6 (b)) allows to further reduce the number of hit combinations to take into account, limiting the region of interest to a cone around the seeding track, such that the track extrapolated position to the hit surface is compatible with the hit position in 3 standard deviations.

For each seeding track a collection of hit pairs satisfying the above requirements is identified and used to construct the trajectory seeds, i.e. the proto-tracks providing the initial kinematic parameters needed for the trajectory propagation. At least three points are requested to evaluate the 5 parameters of the initial kinematic, but only two hits are provided per hit pair, and some of them have a coarse resolution in the z coordinate. The third measurement is provided, again, by the estimated position of the conversion vertex (C). The coordinates of these three points in the (x, y) plane allow to estimate the p_T of the trajectory seed. The direction of the trajectory seed in the (z, r) plane is imposed parallel to the seeding track.

Seeds are then propagated outward, adding compatible hits and updating the trajectory until either the detector boundary is reached, or no additional compatible hits can be found. In the final stage, the collection of hits is fit to obtain the best estimate of the track parameters.

6. Results

The impact of the dedicated tracking algorithm to the reconstruction of photon conversions can be seen on Fig. 7 showing the contribution of the different tracking steps to the photon conversion reconstruction as estimated by the simulation for a detector region $|\eta| < 1$. The additional step increases by more than a factor two the number of conversions at large radii – outside the Pixel detector region – and contributes significantly ($\sim 20\%$) in the Pixel detector

layers. At the same time the additional number of reconstructed fake photon conversions is kept low (Fig. 7 (b)), thanks to the demanding geometrical requirements adopted.

Table 1 summarises the reconstruction performance of our algorithm in terms of the increased number of true and fake photon conversions, distinguishing among barrel and endcap regions as well as among conversions undergone in the Pixel detector ($r < 15$ cm) or in the remaining Tracker volume.

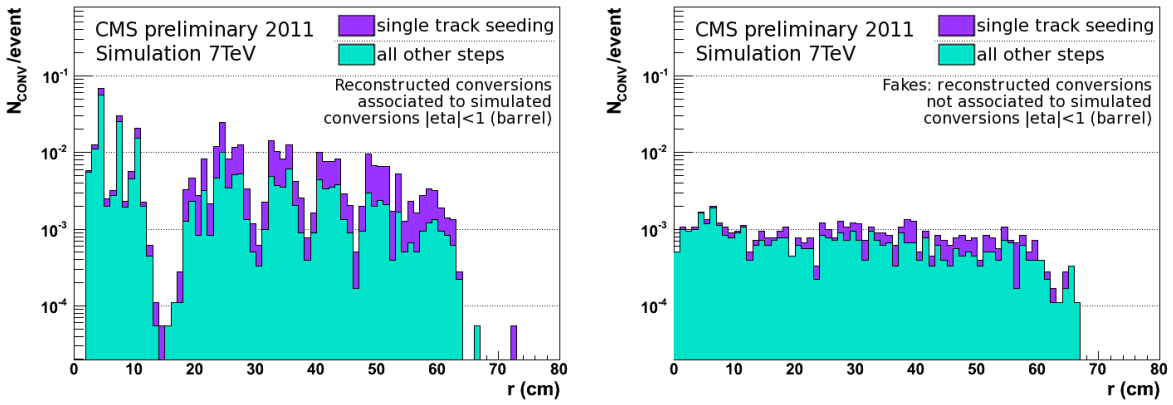

(a) (b)

Figure 7. Fraction of the reconstructed true (a) and fake (b) photon conversions per event as a function of the radial position of the conversion vertex, for $|\eta| < 1$, as estimated from simulation. The different colors correspond to the standard reconstruction algorithms only (green) and to the contribution of the new reconstruction algorithm (purple).

Table 1. Reconstruction performance of the dedicated algorithm in terms of the increase fraction of true and fake photon conversions, distinguishing among barrel and endcap regions as well as among conversions undergone in the Pixel detector ($r < 15$ cm) or in the remaining Tracker volume.

	Sim & Reco conversions		Fake conversions	
radius [cm]	< 15 cm	≥ 15 cm	< 15 cm	≥ 15 cm
barrel	+20%	+200%	+5%	+28%
endcap	+26%	+83%	+11%	+67%

In the overall increase of reconstruction efficiency we account also the improved efficiency in the transition region between the Tracker barrel and endcap. Figure 8 shows the reconstruction efficiency as a function of the conversion vertex position in the (z, r) plane, evaluated with simulated data using only the standard CMS algorithms (Fig. 8 (a)) or including our dedicated algorithm (Fig. 8 (b)). An increase of efficiency is visible in the less populated area around $|\eta| \sim 1.2$ when the dedicated algorithm is adopted. This improvement is extremely useful to determine the amount of material in the transition region as well as to increase the detector acceptance for physics studies.

Figure. 9 shows the reconstruction efficiency enhancement due to the dedicated algorithm as a function of the transverse momentum of the produced lepton tracks. The algorithm contributes

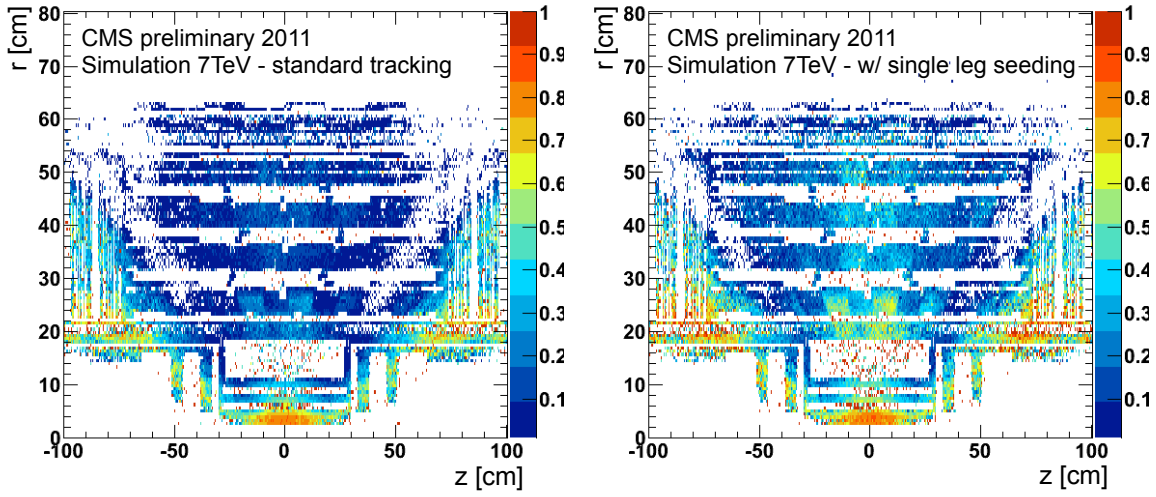

(a) (b)

Figure 8. Reconstruction efficiency as a function of the conversion vertex position in the (z, r) plane, evaluated with simulated data using only the standard CMS algorithms (a) or including the dedicated conversion algorithm (b).

to reconstruct mainly the low p_T tracks, whereas the leading track is, by design, reconstructed by the standard algorithms.

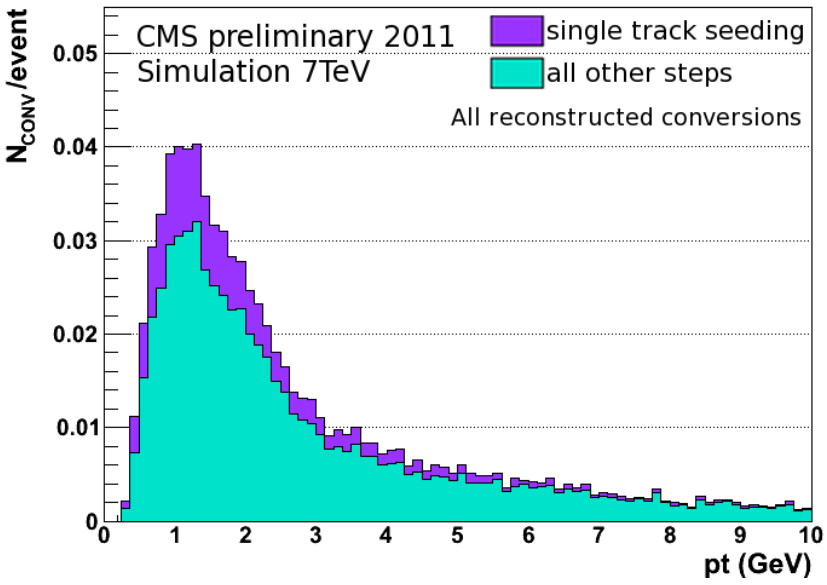

Figure 9. Fraction of simulated and reconstructed photon conversions as a function of the transverse momentum of the produced lepton tracks, using only standard tracking algorithms (green) or also the dedicated algorithm (purple).

In terms of processing time per event, this dedicated tracking sequence fits well the available time quota imposed by the reconstruction constraints in the LHC high luminosity environment. The good time performance is again a consequence of the demanding requirements applied

to limit the number of combinations to examine. Moreover some of the topological concepts exploited by our algorithm have been adopted also to optimize the processing time of the standard photon conversion reconstruction in CMS, allowing to gain a factor of 15 in processing time with a smarter preselection of the tracks to be paired [8]. This preselection is built on the same criteria used to identify the expected position of a conversion vertex from a single track. It avoids to pair a track with all the opposite-charge tracks before rejecting it as not compatible with a conversion in the Tracker material.

7. Conclusions

The photon conversions in the detector material is not just a nuisance in the event reconstruction of HEP experiments, but can also be extremely useful. We have developed in CMS a dedicated tracking for photon conversions that, exploiting their topology, enhances the reconstruction efficiency by a factor of 20% to 200% depending on the radial distance from the beamline.

References

[1] R. Adolphi et al. The CMS experiment at the CERN LHC. *JINST*, 0803:S08004, 2008.

[2] Steve Wasserbaech. Computeraized tomography of the ALEPH detector. *ALEPH Internal Note*, ALEPH 97-08, 1997.

[3] CMS Collaboration. Studies of tracker material. *CMS Physics Analysis Summary*, TRK-10-003, 2010.

[4] CMS Collaboration. Observation of the χ_c states with 1.1 fb^{-1}. *CMS Detector Performance Summaries*, CMS-DP-2011-011, 2011.

[5] CMS Collaboration. Photon reconstruction and identification at $\sqrt{s}$=7 TeV. *CMS Physics Analysis Summary*, CMS-PAS-EGM-10-005, 2010.

[6] CMS Collaboration. Tracking and vertexing results from first collisions. *CMS Physics Analysis Summary*, TRK-10-001, 2010.

[7] K. Nakamura et al. (Particle Data Group). The review of particle physics. *J. Phys. G*, 37, 2010.

[8] D. Giordano and G. Sguazzoni. CMS reconstruction improvements for the tracking in large pile-up events. *Journal of Physics Conference Series*, CHEP2012, 2012.